chemistry

MDPI

Article

Investigation of the Properties of Mo/ZSM-5 Catalysts Based on Zeolites with Microporous and Micro–Mesoporous Structures

Andrey A. Stepanov *, Ludmila L. Korobitsyna and Alexander V. Vosmerikov

Institute of Petroleum Chemistry SB RAS, 634055 Tomsk, Russia; kll@ipc.tsc.ru (L.L.K.); pika@ipc.tsc.ru (A.V.V.)
* Correspondence: stepanov@ipc.tsc.ru

Abstract: The dehydroaromatization of methane (MDA) is of great interest as a promising process for processing natural and associated petroleum gases, the main component of which is methane. The rapid loss of catalyst activity because of coke formation hinders the introduction of the DHA methane process into the industry. Therefore, the aim of this research was to find ways to improve Mo/ZSM-5 catalysts for MDA. The paper presents the results of the synthesis of high-silica zeolites of the ZSM-5 type with microporous and micro–mesoporous structures, the preparation of Mo/ZSM-5 catalysts based on them, and the study of the physicochemical and catalytic properties of the obtained samples during the non-oxidative conversion of methane into aromatic hydrocarbons. Zeolite catalysts were investigated using IR spectroscopy, X-ray diffraction, TPD-NH_3, SEM, HR-TEM, and N_2 adsorption. It was found that the addition of carbon black in the stage of the synthesis of zeolite type ZSM-5 did not lead to structural changes, and the obtained samples had a crystallinity degree equal to 100%. The creation of the micro–mesoporous structure in Mo/ZSM-5 catalysts led to an increase in their activity and stability in the process of methane dehydroaromatization. The highest conversion of methane was observed on a 4.0%Mo/ZSM-5 catalyst prepared based on zeolite synthesized using 1.0% carbon black and was 13.0% after 20 min of reaction, while the benzene yield reached 7.0%. It was shown using HR-TEM that a more uniform distribution of the active metal component was observed in a zeolite catalyst with a micro–mesoporous structure than in a microporous zeolite.

Keywords: methane dehydroaromatization; zeolite ZSM-5; micro–mesoporous structure; benzene

check for updates

Citation: Stepanov, A.A.; Korobitsyna, L.L.; Vosmerikov, A.V. Investigation of the Properties of Mo/ZSM-5 Catalysts Based on Zeolites with Microporous and Micro–Mesoporous Structures. *Chemistry* **2023**, *5*, 1256–1270. https://doi.org/10.3390/chemistry5020085

Academic Editors: Tetsuya Satoh and Koji Hirano

Received: 21 April 2023
Revised: 15 May 2023
Accepted: 15 May 2023
Published: 17 May 2023

Copyright: © 2023 by the authors. Licensee MDPI, Basel, Switzerland. This article is an open access article distributed under the terms and conditions of the Creative Commons Attribution (CC BY) license (https://creativecommons.org/licenses/by/4.0/).

1. Introduction

The development of effective methods for processing natural and associated petroleum gases into fuel and valuable chemical products has been an urgent research area for decades [1–6]. Huge reserves of natural gas (4036.9 trillion m^3) [7], as well as recent achievements in the field of shale gas production, force researchers to develop new methods and improve existing ones for processing methane as the main component of natural gas. Natural gas is a mixture of methane (70–98%), ethane, propane, butane, pentane, and other components. In addition, methane is the main component of associated petroleum and shale gases, biogas, and gas hydrates, the so-called unconventional resources. Therefore, the problem of processing natural hydrocarbon gases is primarily the problem of methane processing.

Despite the huge reserves of natural gas, its use as a chemical raw material remains low. There are still no direct ways to convert methane into chemical products and fuel. Currently, natural gas is mainly burned to generate electrical and thermal energy, and only 5% of natural gas is sent for chemical processing, of which 70% is to produce ammonia; a total of 20% is for the synthesis of methanol; and the rest is used to produce various chemicals [8].

One of the promising directions of natural gas processing is the process of the non-oxidative conversion of methane into aromatic hydrocarbons (MDA: $6\ CH_4 \leftrightharpoons C_6H_6 + 9\ H_2$) on high-silica zeolites (HSZs) modified with various transition metals [2,8–13]. The target product of MDA

is benzene—one of the most popular chemical products. Benzene is the most important raw material for the chemical industry, since it is used both as a starting reagent for the synthesis of a wide variety of compounds and as a solvent for other reactions. The Mo/ZSM-5 catalytic system exhibits the highest activity and stability during the conversion of methane into aromatic hydrocarbons [2,14–18]. It is well known that Mo-containing zeolites are bifunctional catalysts. Methane is first activated on the metal centers of the catalyst with the formation of hydrogen and lower olefins; then, the aromatization process proceeds on the acid centers of the zeolite itself by means of proton transfer, oligomerization, and dehydrocyclization with the formation of benzene. Consequently, zeolite acid centers play an important role in the formation of benzene from methane on Mo/ZSM-5 catalysts. It was found that when the Mo/ZSM-5 catalyst is calcined at a temperature of 350 °C, the formation of MoO_x particles can be localized on the external surface of the zeolite. An increase in the calcination temperature to 500–700 °C leads to the migration of molybdenum oxide particles into the zeolite channels and interaction with its Brönsted acid centers (BACs). In the first minutes of the MDA reaction, a mixture of Mo_2C and MoO_xC_y particles is formed, which are active in this process [11,14,16,18]. However, narrow zeolite channels formed by micropores complicate the mass transfer process and contribute to intensive coke formation and thus a rapid drop in catalyst activity. Obtaining catalysts based on zeolites with a micro–mesoporous structure is an urgent problem and opens new possibilities for their application [19,20]. In recent years, the attention of many research groups has been directed to the creation of zeolite-containing catalysts with an additional mesoporous structure [19,21–26]. The synthesis of zeolite of the ZSM-5 type with an ordered hierarchical pore system is a promising direction for obtaining a catalyst with higher activity and stability in the methane dehydroaromatization reaction than microporous zeolite. On the one hand, the modification of the zeolite carrier with the formation of secondary mesoporosity leads to improvement in the dispersion of the active component and an increase in the availability of active catalyst centers, which is of great importance for the effective course of the methane dehydroaromatization reaction. On the other hand, the combination of micro- and mesopores in the structure of the zeolite carrier facilitates the diffusion of reagents to the active centers inside the zeolite channels and the products formed from them, which makes it possible to increase the activity of the metal-containing zeolite catalyst and reduce the intensity of coke formation on its surface.

In this regard, the purpose of this work was to develop methods for the synthesis of zeolites of the ZSM-5 type with a micro–mesoporous structure using the second template of carbon black and the preparation of Mo-containing catalysts based on them and to study the physicochemical and catalytic properties of the obtained zeolite-containing systems in the process of methane dehydroaromatization.

2. Materials and Methods

Synthesis of zeolites. High-silica zeolites (HSZs) with a micro–mesoporous structure were obtained with hydrothermal synthesis using hexamethylenediamine and carbon black as structure-forming agents. Carbon black of grade P354, obtained from Institute of Hydrocarbon Processing Problems SB RAS (Omsk), has the following composition: C—96.4%; O—2.5%; S—0.5%; N and H—0.3%; specific surface area—110 m^2/g. Carbon particles are homogeneous and have a globular shape with sizes from 30 to 60 nm. A feature of carbon black is the presence of photogenic functional groups on its surface—ion adsorption centers. Oxygen in the composition of carbon black is in hydroxyl, carbonyl, ether, and carboxyl groups. Before use, carbon black was pre-activated for 1 h while stirring in 1 M NaOH solution at room temperature, after which it was dried at a temperature of 100 °C.

A carbon template was added to alkaline alumina–silica gel in amounts of 0.5–5.0 wt%, based on the mass of the resulting zeolite. A solution of sodium silicate (liquid glass composition) was used to prepare alkaline alumina–silica gel, with 19.0% SiO_2 and 7.2% Na_2O. Hexamethylenediamine (HMDA) was used as a structure-forming agent. The

resulting reaction mass was placed in a steel autoclave with Teflon liner and kept at a temperature of 170 °C for 4 days. The resulting reaction mixture corresponded to the following molar composition: Al_2O_3: 40 SiO_2: 5.4 HMDA: 15 Na_2O: 2200 H_2O: 2 C.

After the synthesis was completed, the crystalline solid phase was filtered with a Buchner funnel, washed with distilled water to achieve pH = 7, dried at 100 °C for 6 h and calcined at 550 °C for 6 h to remove organic and carbon templates. The sodium form of zeolite obtained after crystallization was converted into the ammonium form using treatment with a 25% solution of ammonium chloride at 90 °C for 2 h under constant stirring. After ion exchange, the zeolite was filtered using a Buchner funnel, washed with distilled water, and dried at 100 °C for 6 h. To obtain the hydrogen form of zeolite, the ammonium form was calcined at 550 °C for 6 h.

The synthesized ZSM-5 zeolites have the following designations: ZSM-5—without the use of a carbon template; ZSM-5/0.5-5.0—with the addition of 0.5–5.0 wt% carbon black.

Catalyst preparation. Catalysts of 4%Mo/ZSM-5 were prepared with the dry mechanical mixing of zeolites in H-form with nanoscale Mo powder obtained with the method of the electric explosion of a conductor in argon medium. The Mo content in the catalysts was 4.0 wt%. The average particle size of Mo was 70–110 nm. The resulting samples were calcined at a temperature of 550 °C for 4 h. The prepared catalysts have the following designation: Mo/ZSM-5—without using a carbon template; Mo/ZSM–5/0.5–5.0—with the addition of 0.5–5.0 wt% carbon black.

Catalyst characterization. The quality of the synthesized zeolites was monitored using IR spectroscopy and X-ray diffraction (XRD) methods. The IR spectra of the samples were obtained using a Nicolet 5700 IR Fourier spectrometer (Thermo Electron Corporation, Waltham, MA, USA) in the region of 4000–400 cm^{-1}. The degree of crystallinity was determined with the method described in [27]. The samples were not subjected to heat treatment before analysis.

The chemical composition of the samples was analyzed using an «EDX-800HS» (Shimadzu, Kyoto, Japan) energy dispersive X-ray fluorescence spectrometer with a Rh anode X-ray tube (voltage of 15–50 kV, current of 20–1000 μA, vacuum, and collimator of 3–5 mm) and a PFA-378 flame photometer.

The phase composition and degree of crystallinity of the samples were assessed using X-ray diffraction (XRD). Before analysis, the samples were heat-treated at 550 °C for 4 h to remove the template. Diffraction patterns were recorded with a «DISCOVER D8» (Bruker, Karlsruhe, Germany) diffractometer equipped with a Lynx-Eye detector using monochromatic CuKα radiation. Scanning was carried out in the range of angles 2θ = 6–90°; the scan step was 0.02 degrees; and the accumulation time was 3 s. The relative degree of crystallinity was calculated from the ratio of the total integrated intensity from the crystalline phase to the sum of the total integrated intensity from the crystalline and amorphous phases. X-ray phase analysis was performed using the PDXL software package by comparing the obtained diffraction patterns with the PDF2 database.

The morphology and crystal size of the samples were investigated using scanning electron microscopy (SEM) with a «JEOL JSM-6490LV» (JEOL, Tokyo, Japan) electron microscope. The SEM images were recorded in secondary electron mode at an accelerating voltage of 20 kV and a working distance of 10 mm. Before recording, the samples were placed on the surface of a 25 mm diameter aluminum table and fixed with conductive adhesive tape.

The study of the structure and microstructure of the samples was carried out using high–resolution transmission electron microscopy (HR-TEM) with an electron microscope, «ThemisZ» (Thermo Fisher Scientific, Waltham, MA, USA), with accelerating voltage of 200 kV and maximum resolution of 0.07 nm and in the scanning mode of electrons scattered at large angles (HAADF STEM) [28]. The images were recorded using a Ceta 16 CCD matrix (Thermo Fisher Scientific). The device was equipped with an energy dispersive spectrometer of X-ray characteristic radiation (EDS), Super (Thermo Fisher Scientific), with a semiconductor Si detector with energy resolution of 128 eV.

The acidic properties of the obtained catalysts were studied with the method of the thermoprogrammed desorption of ammonia (TPD-NH_3), which makes it possible to determine the number and the strength distribution of acid sites [29]. The samples were loaded into a quartz tubular reactor, were pretreated under Ar flow at 600 °C for 1 h, and then cooled down to 50 °C. The adsorption of ammonia was carried out at 100 °C until the sample was completely saturated; then, the physically adsorbed ammonia was removed using helium purging at the same temperature for 2 h, after which desorption was carried out in the temperature range 100–550 °C at a temperature rise rate of 10 °C/min.

The characteristics of the porous structure were determined with the method of the low-temperature adsorption–desorption of nitrogen (77 K) with an «ASAP-2020» sorbtometer (Micromeritics, Norcross, GA, USA). Before analysis, the samples were evacuated at 350 °C for 6 h. The specific surface area was calculated with the BET method at relative partial pressure $P/P_0 = 0.2$. The pore size distribution was calculated from the desorption curve using the BJH method (Barrett–Joyner–Halenda). The total pore volume was determined using the BJH method at relative partial pressure $P/P_0 = 0.95$, while the volume of micropores in the presence of mesopores was determined using the t method by Lippens and de Boer.

Catalytic evaluation. The process of the non-oxidative conversion of methane (99.99% purity) was investigated in a flow-through reactor at 750 °C, a volumetric feed rate of 1000 h^{-1}, and atmospheric pressure. A quartz reactor was charged with 1 cm^3 of catalyst (fractional composition: from 0.5 to 1.0 mm). At first, the catalyst was heated in He current to 750 °C and kept at this temperature for 20 min. To prevent the condensation or strong adsorption of high-boiling hydrocarbons formed during the reaction, the tube at the outlet of the reactor and the six-way tap for sampling for analysis were thermostated at a temperature of 240 °C [30]. The reaction products were analyzed with gas–liquid chromatography using a «Chromatek-Kristall 5000.2» (Chromatek, Yoshkar-Ola, Russia) chromatographer every 40 min during the catalytic experiment. To assess the catalytic properties of the samples, the degree of methane conversion, the yield, and the selectivity of the formation of reaction products were determined.

The quantitative calculation of the composition of the resulting reaction products was carried out using the internal normalization method. The method is based on determining the ratios between the concentrations of the components of the mixture. The calculation consists in bringing to 100% the products of the peak width at half height by the height of all the peaks of the chromatogram.

Formulas are used for this:

$$C_i = \frac{k_i \times h_i \times l_i}{\sum k_i \times h_i \times l_i} \times 100\%, \quad (1)$$

where C_i is the concentration of the i-th component in the gas phase, wt%; k_i is the coefficient determined by the sensitivity of the detector to this component; h_i is the height of the i-th peak; and l_i is the half width of the i-th peak.

The conversion of methane was calculated using the following formula:

$$X = \frac{M - m_{prod.}}{m_{feedstock}} \times 100\%, \quad (2)$$

where M is the total concentration of reaction products; $m_{prod.}$ is the concentration of methane in the reaction products; and $m_{feedstock.}$ is the concentration of methane in the feedstock.

The selectivity of the i-th component is calculated with the following formula:

$$S_i = \frac{m_i}{X}, \quad (3)$$

where m_i is the concentration of the i-th component in the reaction products and X is the conversion of methane.

3. Results

IR spectroscopy. Figure 1 shows the IR spectra of non-calcined zeolites with a high degree of crystallinity obtained without and with the addition of carbon black in the synthesis of the reaction mixture.

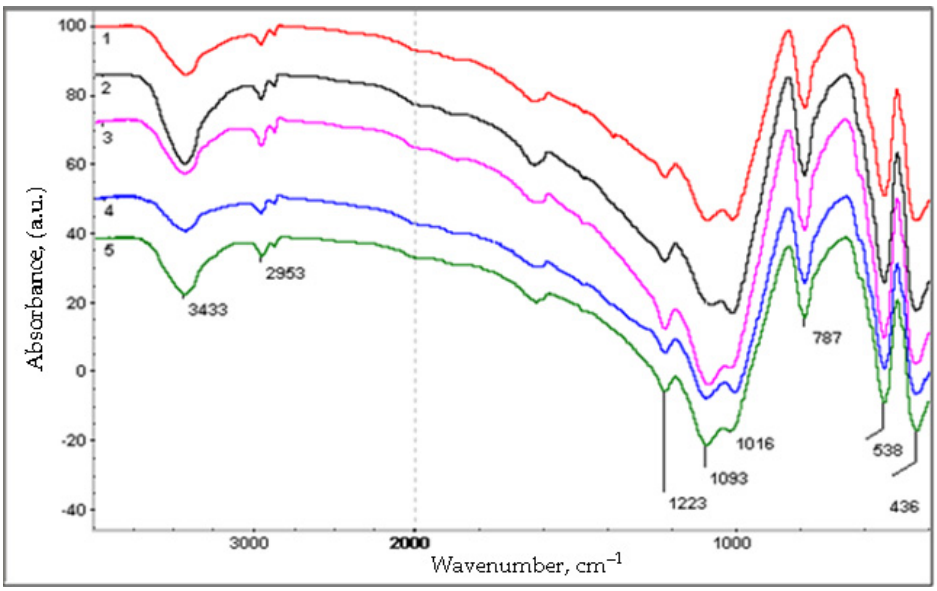


Figure 1. IR spectra of ZSM-5 zeolites synthesized with carbon-free template (1) and with the addition of carbon black in the amounts of 1.0 (2), 2.0 (3), 3.5 (4), and 5.0% (5).

Absorption bands at 436, 538, 787, and 1093 cm^{-1} characteristic of ZSM-5 were observed in the IR spectra [31]. The bands at 436 and 1093 cm^{-1} refer to vibrations inside the SiO_4 and AlO_4 tetrahedra and are not responsible for the zeolite structure. The wide intense absorption band in the region of 950–1200 cm^{-1} refers to the antisymmetric valence vibrations of SiO_4 and AlO_4, and the absorption band at 436 cm^{-1} refers to deformation vibrations inside the SiO_4 and AlO_4 tetrahedra. The absorption band at 787 cm^{-1} is associated with valence vibrations of SiO_4 and AlO_4 tetrahedra. The absorption band at 538 cm^{-1}, which relates to fluctuations in the external bonds of the Al and SiO_4 tetrahedra of the frame, is due to the presence of double four- and six-membered rings in the frame and determines the structure of the zeolite. The presence of this band in the infrared spectrum of zeolite indicated that it belonged to the ZSM-5 type. On the IR spectrum, there was an absorption band in the region of 2953 cm^{-1}, related to the C-H bonds of hexamethylenediamine. The ratio of the intensities of the absorption bands at 538 and 436 cm^{-1} allowed us to judge the purity of the synthesized samples and the degree of their crystallinity. The crystallinity of all synthesized zeolites was 100%.

XRD. The obtained zeolites were studied with the X-ray phase method. Figure 2 shows the diffractograms of zeolites synthesized both without the addition of carbon black and using a carbon template. All samples were characterized by the presence of well-resolved peaks in the range of angles 2θ = 6–34°, which indicated their belonging to the zeolite type of ZSM-5 [31]. The absence of traces of impurity phases (quartz—26.7°; cristobalite—22.0°) and the broadening of the peak lines indicated a high degree of crystallinity of the synthesized zeolites, equal to 100%.

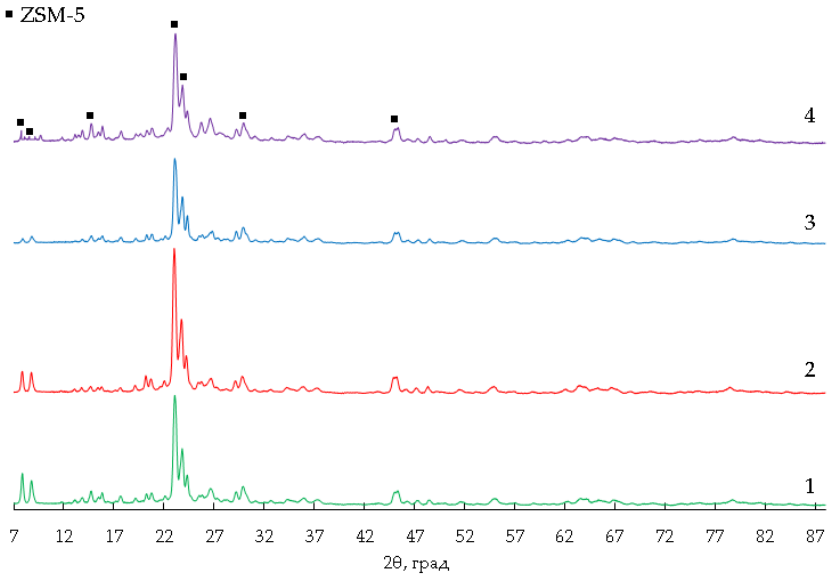


Figure 2. XRD patterns of ZSM-5 synthesized without the addition of carbon template (1) and with the addition of carbon black in the amounts of 1.0 (2), 3.5 (3), and 5.0% (4).

Thus, the studies of zeolites using IR spectroscopy and X-ray phase analysis showed that the addition of a carbon template during the synthesis of zeolites did not affect their structural properties, and all synthesized zeolites belonged to the ZSM-5 type and had a high degree of crystallinity.

Chemical composition. The studies of the chemical composition of the obtained zeolites using X-ray fluorescence analysis showed that their silicate modulus (SiO_2/Al_2O_3) was 40 (Table 1). Thus, the addition of a carbon template during the synthesis of zeolite did not affect its silicate module.

Table 1. Chemical analysis of synthesized zeolites.

Zeolite	Element Content, Mass %			
	Si	O	Al	* M
ZSM-5	49.09	45.90	2.46	2.55
ZSM-5/1.0	54.65	42.40	2.77	0.18

*—Fe, Mg, Ca, and Ni.

The Mo contents in catalysts Mo/ZSM-5 and Mo/ZSM-5/1.0 were 3.89 and 3.90%, respectively. The observed slight decrease in the concentration of Mo was associated with losses during the mechanical mixing of zeolite and nanoscale Mo powder, as well as sublimation during the calcination of the catalysts. The Na content in all the zeolites studied was 0.04%.

SEM. Figure 3 shows electron microscopic images of the synthesized zeolites. Zeolite particles synthesized without the addition of carbon black were homogeneous in their composition and had the form of polycrystalline spheroids with sizes from 6 to 8 microns (Figure 3a). In the electronic image of zeolite synthesized with the addition of carbon black in the amount of 1.0%, a looser connection (disassembly) of crystals in polycrystalline spheroids was observed; while they were less homogeneous, the size of the crystals varied from 4 to 8 microns (Figure 3b). When the carbon black content in the reaction mixture increased to 3.5% during the synthesis of zeolite and its subsequent calcination, inhomogeneous particles were formed (Figure 3c). The size of polycrystalline spheroids varied from 4 to 9 microns; in addition, the formation of larger particles with sizes up to 12 microns was observed.

Thus, with an increase in the concentration of carbon black added during the synthesis of zeolite from 1.0 to 5.0%, the number of inhomogeneous zeolite crystals formed increased, and their size increased.

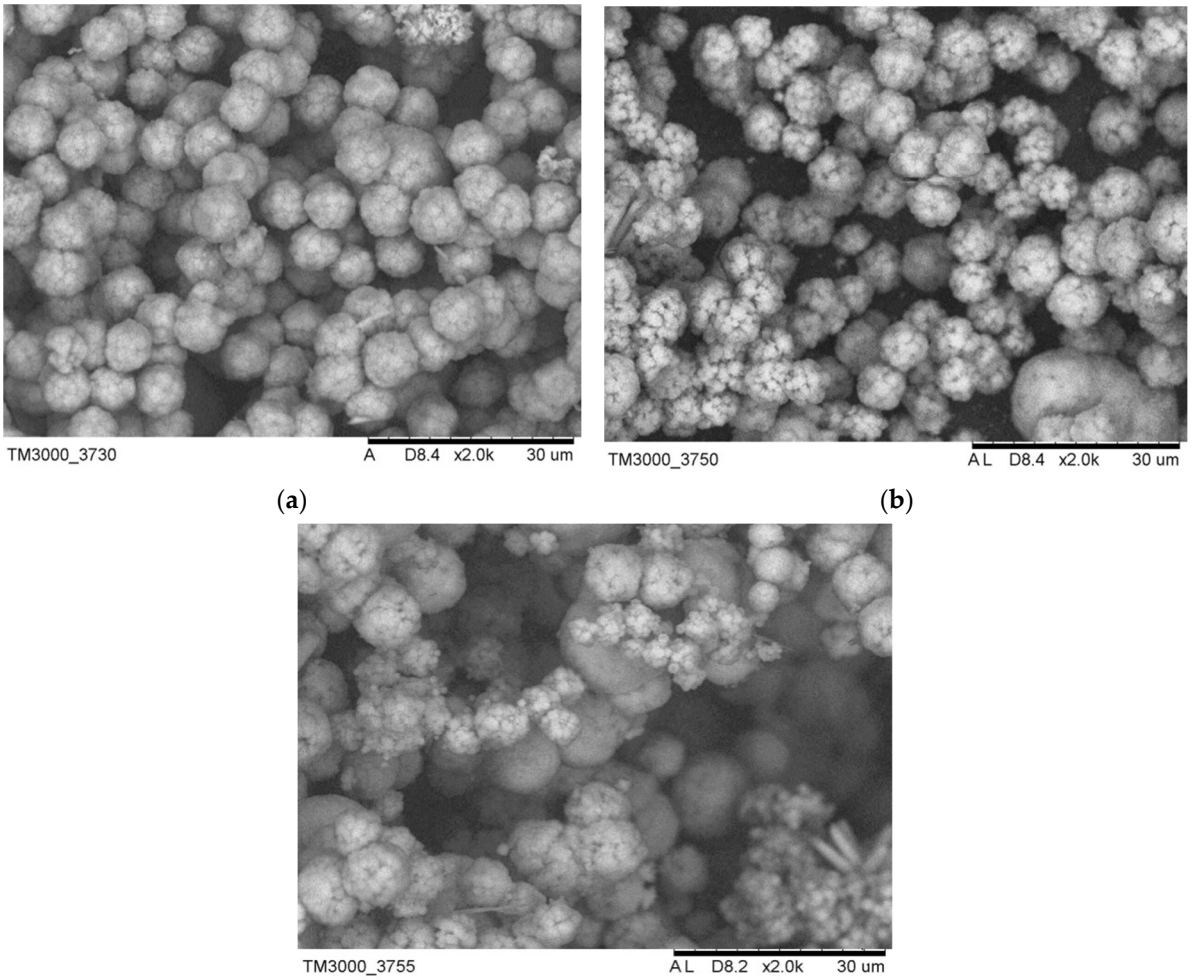


Figure 3. SEM images of ZSM-5 zeolites synthesized without the addition of carbon template (**a**) and with the addition of carbon black in the amounts of 1.0% (**b**) and 3.5% (**c**).

TPD-NH_3. Since the metal-containing zeolite catalysts of MDA have a bifunctional nature associated with the presence of both metallic active centers and acidic zeolite centers, it was of interest to investigate the acidic characteristics of micro–mesoporous zeolites and the catalysts derived from them [32].

Figure 4 shows the thermal desorption spectra of ZSM-5 zeolites synthesized without and with a carbon template. On all curves, there were two peaks with clearly defined temperature maxima in the regions of 180–200 °C and 430–440 °C, indicating the presence of two types of acid centers—weak and strong. Strong acid centers mainly belong to Brönsted acid centers, which are responsible for the formation of aromatic hydrocarbons [33,34].

The intensity of the high-temperature peak in the region of 430–460 °C for zeolites synthesized with the addition of carbon black was slightly weaker than that for ZSM-5 zeolite, which was associated with a decrease in the number of BACs.

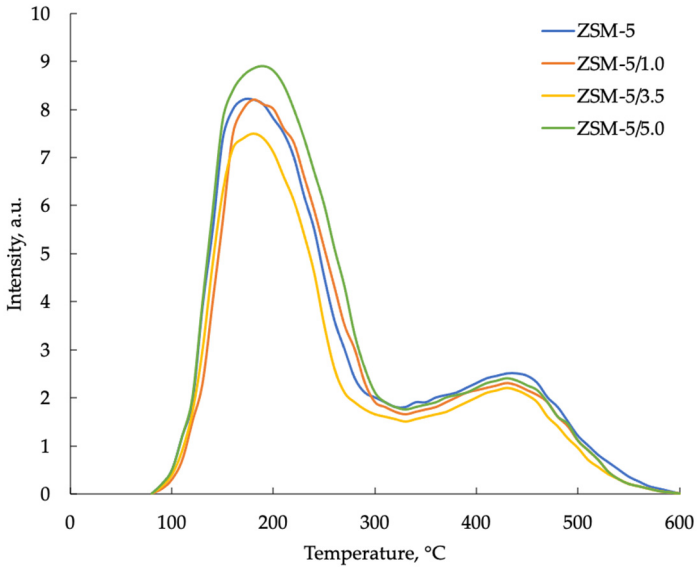


Figure 4. TPD profiles of ZSM-5 zeolites.

The addition of 1.0% carbon black in the stage of zeolite synthesis practically did not affect its acidity (Table 2). The concentrations of strong acidic centers of zeolites obtained without and with the addition of 1.0% carbon black were 388 and 389 mmol/g, respectively. An increase in the concentration of carbon black in the composition of the reaction gel to 5.0% led to a decrease in the content of strong acid centers in zeolite to 322 mmol/g and to an increase in the concentration of its weak acid centers to 824 mmol/g. This change was probably due to the fact that the addition of carbon in the stage of zeolite synthesis led to differences in the distribution of Al atoms in the zeolite structure, i.e., there was a change in the ratio of Lewis and Brönsted acid centers. At the same time, the total concentration of acidic zeolite centers with the addition of carbon black practically did not change and reached 1146 mmol/g.

Table 2. Acid characteristics of zeolites and catalysts.

Sample	T, °C		Concentration, μmol/g		
	T_I	T_{II}	C_I	C_{II}	C_Σ
ZSM-5	185	440	753	388	1141
4%Mo/ZSM-5	180	430	807	355	1162
ZSM-5/1.0	185	435	767	389	1156
ZSM-5/2.0	180	430	787	364	1151
ZSM-5/3.5	185	430	793	348	1141
ZSM-5/5.0	195	435	824	322	1146
4%Mo/ZSM-5/1.0	160	430	810	315	1125

Note. T_I and T_{II} are the temperatures of peak maxima for "weak" and "strong" acid centers, respectively. C_I, C_{II}, and C_Σ—concentrations of "weak" and "strong", and total concentration of acid centers, respectively.

The addition of Mo to microporous ZSM-5 zeolite led to a decrease in the strength and concentration of strong acid centers from 388 to 355 mmol/g. The decrease in acidity was associated with the interaction of Mo and the Brönsted acid centers of zeolite. The modification of Mo of zeolite synthesized with the addition of 1.0% carbon black led to a more significant decrease in the concentration of strong acid centers, which was due to a more uniform distribution of Mo in the zeolite channels due to the creation of a micro–mesoporous structure [14,32,35].

Table 3 presents the results of the studies of the characteristics of the porous structure of zeolites synthesized without and with the addition of carbon black and Mo/ZSM-5 catalysts.

Table 3. Textural characteristics of zeolites and catalysts.

Sample	S_{BET}, m^2/g	V_{micro}, cm^3/g	V_{meso}, cm^3/g	V_{total}, cm^3/g
ZSM-5	285	0.13	0.02	0.15
4%Mo/ZSM-5	266	0.11	0.02	0.13
ZSM-5/1.0	379	0.12	0.08	0.20
ZSM-5/2.0	378	0.12	0.10	0.22
ZSM-5/3.5	375	0.11	0.11	0.22
ZSM-5/5.0	373	0.11	0.13	0.24
4%Mo/ZSM-5/1.0	343	0.10	0.07	0.17

Note. S_{BET}—specific surface of zeolite measured with the BET method; V_{micro} and V_{meso}—specific volume of micro- and mesopores; V_{total}—total specific volume of pores.

According to the data given in Table 3, the ZSM-5 sample was characterized by a micropore volume of 0.13 cm^3/g and had a specific surface area of 285 m^2/g. When Mo was added to the initial ZSM-5 zeolite, its specific surface area and the volume of micropores decreased, while the volume of macropores did not change. The addition of 1.0% carbon black in the stage of zeolite synthesis led to an increase in its specific surface area and mesopore volume [36]. With an increase in the concentration of carbon black added during the synthesis of zeolite, the total volume of its pores increased because of the formation of mesopores, while the volume of micropores slightly decreased. The addition of Mo to ZSM-5/1.0 zeolite led to a decrease in its specific surface area and total pore volume, and the volume of micropores decreased more significantly than the volume of mesopores, which indicates that molybdenum blocked micropores in zeolite [37].

The presence of mesopores in the synthesized ZSM-5 zeolite was indicated by the characteristic hysteresis loop on the nitrogen adsorption and desorption isotherm shown in Figure 5. At relative pressure P/P_0 equal to 0.4–1.0, for zeolite synthesized using a carbon template, a hysteresis loop was clearly manifested on the adsorption and desorption isotherm of nitrogen.

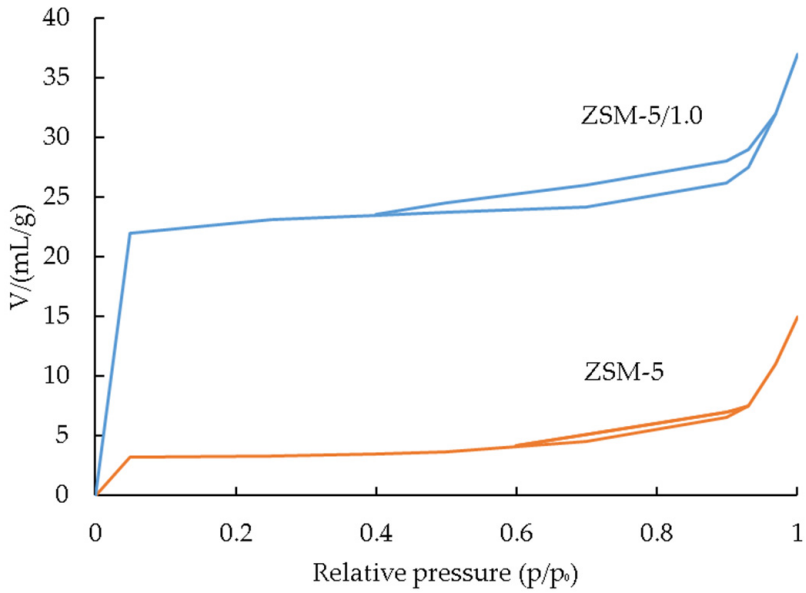


Figure 5. N_2 adsorption and desorption isotherms of ZSM-5 zeolites.

Figure 6 shows data on the pore size distribution in the synthesized zeolites.

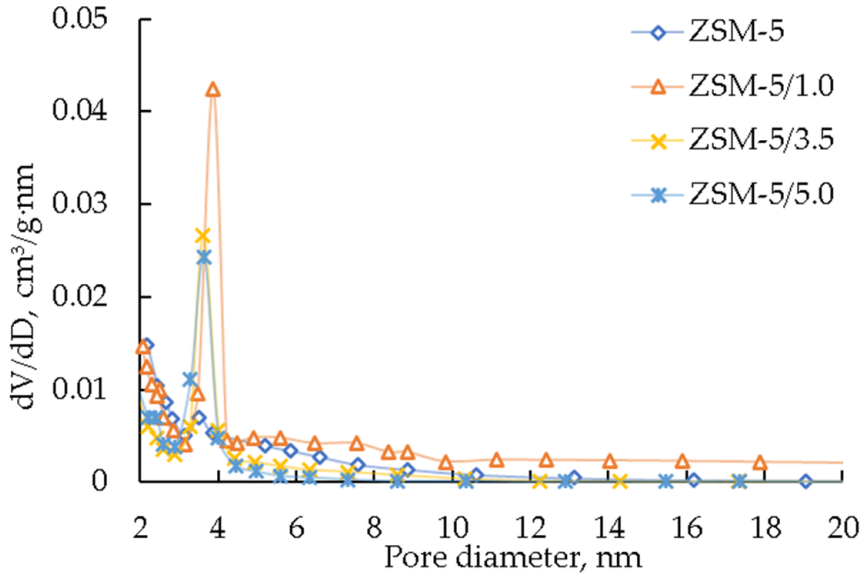
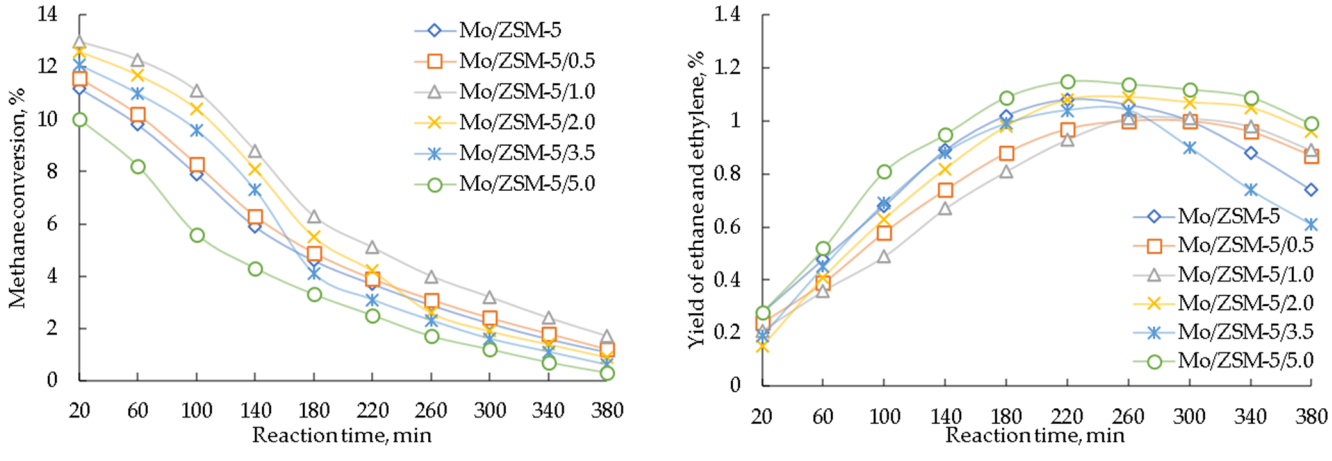


Figure 6. Pore size distribution in zeolites.

For ZSM-5 zeolite synthesized without the addition of a carbon template, the peak in the range of 3–4 nm corresponding to mesopores was practically absent, and only a small shoulder was present. When a carbon template was added in the stage of zeolite synthesis, mesopores were formed, the size of which was 3.5–20.0 nm.

Catalytic results. The results of testing 4%Mo/ZSM-5 catalysts obtained based on zeolites synthesized without and with the addition of various amounts of carbon black in the process of methane dehydroaromatization are shown in Figure 7. In all cases, except for the Mo/ZSM-5/5.0 sample, the use of carbon in the synthesis of zeolite led to obtain a catalyst with higher activity than the Mo/ZSM-5 sample obtained on the basis of zeolite synthesized without the addition of carbon black.



(**a**) (**b**)

Figure 7. *Cont.*

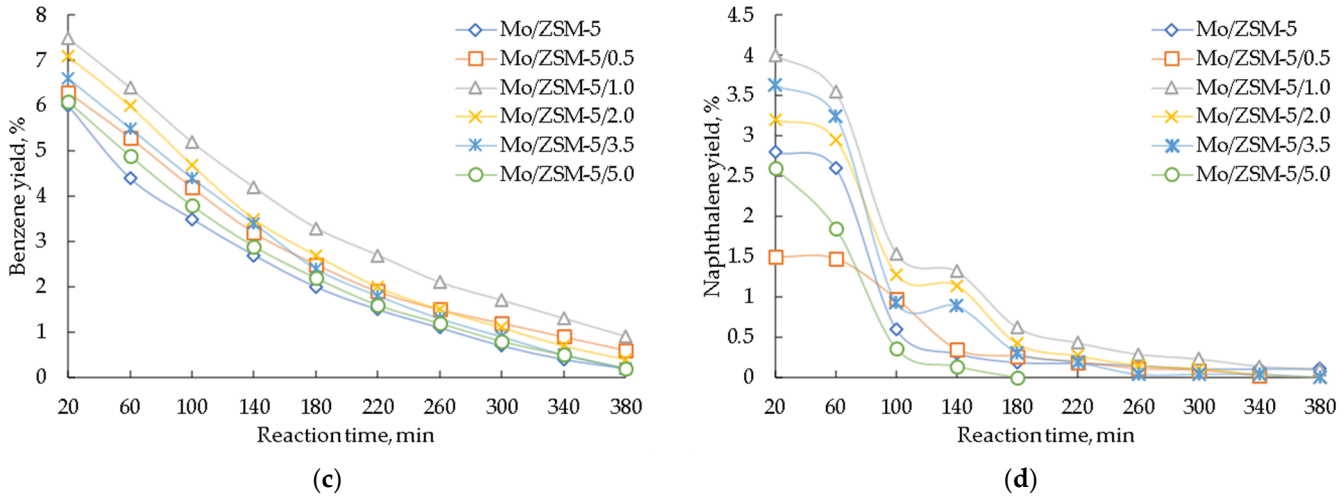


Figure 7. The dependence of the conversion of methane (**a**), the total yield of ethane and ethylene (**b**), benzene (**c**), and naphthalene (**d**) formed on 4% Mo/ZSM-5 catalysts prepared on the basis of zeolite synthesized without and with the addition of various amounts of carbon black on the reaction time.

Micro–mesoporous catalyst Mo/ZSM-5/1.0 showed the greatest activity and stability of operation in the process of MDA (Figure 7a). The conversion of methane on this catalyst was 13% after 20 min of reaction. An increase in the concentration of carbon black to 3.5% led to a decrease in the activity of the Mo-containing zeolite catalyst (conversion of 12.1% after 20 min of reaction); at the same time, its activity during 180 min of reaction was higher than that of the Mo/ZSM-5 sample, after which the conversion of methane approached the conversion methane on the Mo/ZSM-5 catalyst. An increase in the concentration of carbon black to 5.0% led to the production of a Mo-containing catalyst, which was significantly inferior in activity compared with the Mo/ZSM-5 catalyst (the conversion of methane after 20 min was 10%).

The analysis of the composition of gaseous products formed during the conversion of methane showed that they mainly consisted of ethane and ethylene, the yield of which increased as the process proceeded, reaching maximum values in the reaction time interval of 220–300 min, and did not exceed 1.2% (Figure 7b). Then, the concentration of ethane and ethylene decreased because of the carburization of the active centers of Mo-containing zeolite catalysts. Micro–mesoporous zeolite catalysts were characterized by a higher concentration of gaseous products, the largest amount of which was formed on the Mo/ZSM-5/5.0 catalyst.

The composition of liquid methane conversion products contained aromatic hydrocarbons, mainly benzene and naphthalene (Figure 7c,d). The largest amount of benzene was formed in the first 20 min of the reaction on all studied catalysts, after which its yield gradually decreased. The addition of carbon black to the reaction mixture during the synthesis of zeolites led to the production of Mo-containing catalysts, on which a larger amount of benzene was formed. The highest benzene yield was achieved on the Mo/ZSM-5/1.0 sample and was 7.0% after 20 min of reaction. The largest amount of naphthalene was formed over 20–60 min of reaction; then, its yield decreased. The sharpest decrease in naphthalene concentration was observed on the Mo/ZSM-5/5.0 catalyst.

Figure 8 shows the dependence of the selectivity of benzene formation on the operating time of 4%Mo/ZSM-5 catalysts obtained based on zeolites with a micro–mesoporous structure.

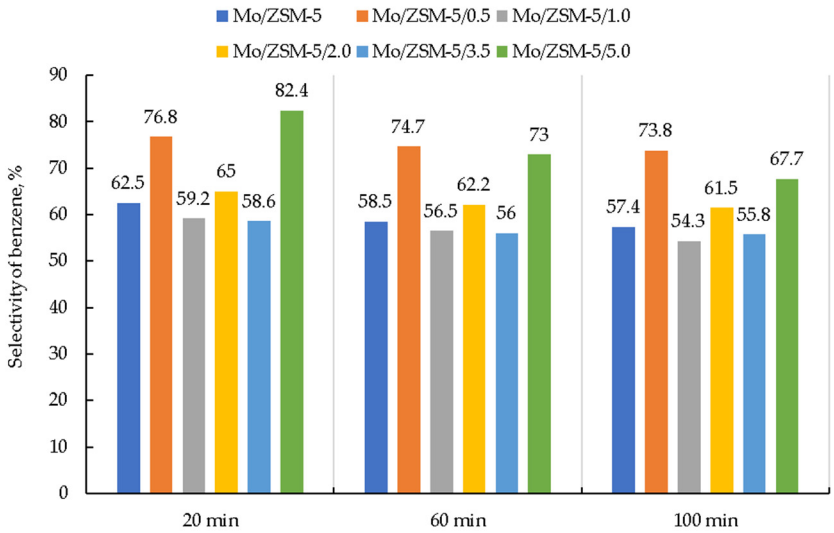
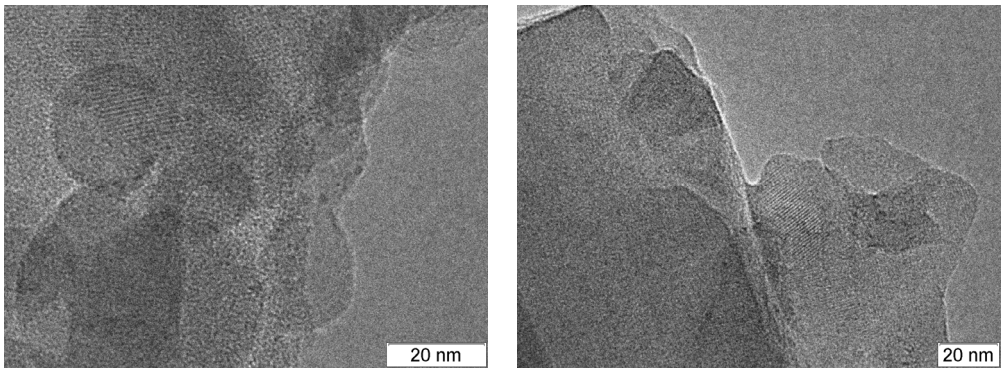


Figure 8. Selectivity of benzene formation on 4%Mo/ZSM-5 catalysts based on zeolites with micro–mesoporous structure.

The greatest selectivity of benzene formation on all studied catalysts was observed in the first 20 min of the reaction. With an increase in the duration of the process, the selectivity of benzene formation on Mo/ZSM-5 catalysts decreased. The highest selectivity of benzene formation was achieved on Mo/ZSM-5 catalysts obtained based on zeolites synthesized with the addition of carbon black in the amounts of 0.5 and 5.0% and reached values of 76.8 and 82.4%, respectively. The selectivity of benzene formation on the microporous Mo/ZSM-5 catalyst during 20 min of reaction was 62.5%.

The difference in the activity of the microporous sample and micro–mesoporous catalysts was probably due to the distribution of the Mo active phase in the zeolite structure. The study of Mo/ZSM-5 catalysts before the MDA process showed that there were no differences in the distribution of Mo. There were no separate Mo components on both catalysts (Figure 9a,b). Only in some cases, nanoparticles of increased contrast were present on the surface of the zeolite, which, according to EDX analysis, belonged to the molybdenum compound, which indicates the molecular dispersed state of the oxidized forms of Mo (Figure 9c).



(**a**) (**b**)

Figure 9. *Cont.*

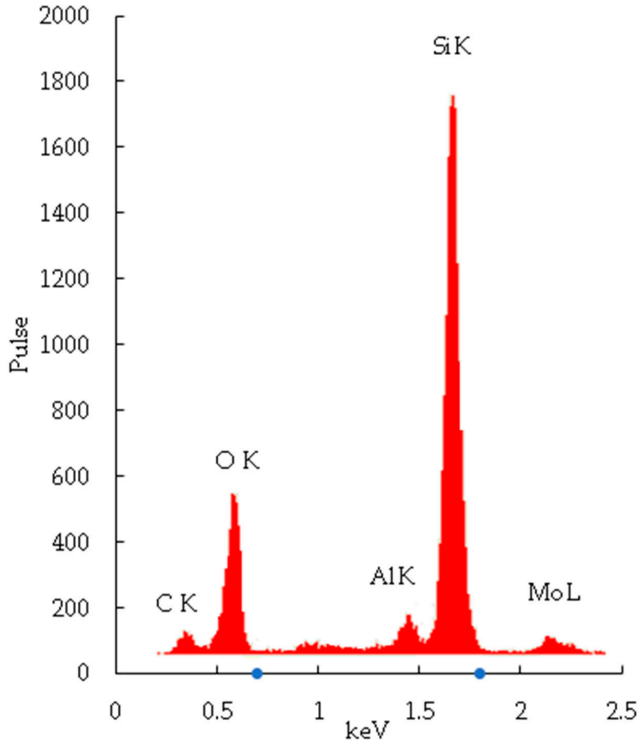
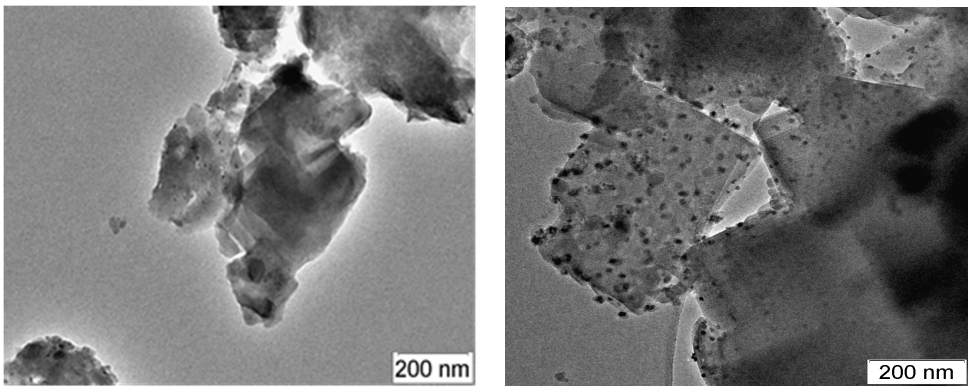


Figure 9. Micrographs of microporous (**a**) and micro–mesoporous (**b**) catalyst 4%Mo/H-ZSM-5 before the MDA process; EDX spectrum obtained from a zeolite site with a microporous structure (**c**).

Figure 10 shows micrographs of Mo/ZSM-5 catalysts based on zeolites with microporous and micro–mesoporous structures, which worked during the dehydroaromatization of methane for 380 min.



(**a**) (**b**)

Figure 10. HR-TEM images of catalysts Mo/ZSM-5 (**a**) and Mo/ZSM-5/1.0 (**b**) after the reaction.

In a catalyst obtained based on microporous zeolite, small clusters of Mo with a size of less than 1 nm were observed in the zeolite channels and particles with a size of up to 10 nm on its surface (Figure 10a). In the 4%Mo/ZSM-5 catalyst prepared using zeolite with a micro–mesoporous structure, there were clusters of Mo of about 1 nm in size with a very dense arrangement in the zeolite channels and particles up to 10 nm in size on the surface, which indicates a more uniform distribution of molybdenum in the zeolite volume (Figure 10b).

4. Conclusions

Thus, the introduction of a carbon template in the stage of the hydrothermal synthesis of zeolite type ZSM-5 led to a change in the size of its crystals and pore volume, with other things being equal under synthesis conditions. According to IR spectroscopy and X-ray diffraction data, the addition of carbon did not lead to structural changes in zeolite, and all synthesized samples belonged to ZSM-5-type zeolite and had a crystallinity degree equal to 100%. In zeolites obtained with the addition of a carbon template, mesopores were present, the largest number of which was in the range of 3–4 nm, and to a large extent, this applied to a sample synthesized with the addition of 1.0% carbon black. It was shown that the Mo-containing catalyst obtained based on ZSM-5 zeolite synthesized with the addition of 1.0% carbon black exhibited the greatest activity and stability in the process of methane dehydroaromatization. The conversion of methane on a 4%Mo/ZSM-5/1.0 catalyst after 20 min of reaction was 13.0%, and the yield of benzene was 7.5%.

Author Contributions: L.L.K. synthesized the zeolites. A.A.S. prepared the catalysts. A.A.S. performed the experimental work. L.L.K., A.A.S. and A.V.V. analyzed the data and wrote the manuscript. All authors have read and agreed to the published version of the manuscript.

Funding: This research was funded by Ministry of Science and Higher Education of the Russian Federation (project No. 121031200182-5).

Data Availability Statement: Not applicable.

Conflicts of Interest: The authors declare no conflict of interest.

References

1. Pinaeva, L.G.; Noskov, A.S.; Parmon, V.N. Prospects for the direct catalytic conversion of methane into useful chemical products. *Catal. Ind.* **2017**, *9*, 283–298. [CrossRef]
2. Ma, S.; Guo, X.; Zhao, L.; Scott, S.; Bao, X. Recent progress in methane dehydroaromatization: From laboratory curiosities to promising technology. *J. Energy Chem.* **2013**, *22*, 1–20. [CrossRef]
3. Taifan, W.; Baltrusaitis, L. CH4 conversion to value added products: Potential, limitations and extensions of a single step heterogeneous catalysis. *Appl. Catal. B Environ.* **2016**, *198*, 525–547. [CrossRef]
4. Horn, R.; Schlogl, R. Methane activation by heterogeneous catalysis. *Catal. Lett.* **2015**, *145*, 23–39. [CrossRef]
5. Majhi, S.; Mohanty, P.; Wang, H.; Pant, K.K. Direct conversion of natural gas to higher hydrocarbons: A review. *J. Energy Chem.* **2013**, *22*, 543–554. [CrossRef]
6. Wang, B.; Albarracin-Suazo, S.; Pagan-Torres, Y.; Nikolla, E. Advances in methane conversion processes. *Catal. Today* **2017**, *285*, 147–158. [CrossRef]
7. BP Statistical Review of World Energy 2022 71st edition. Available online: https://www.connaissancedesenergies.org/sites/default/files/pdf-actualites/bp-stats-review-2022-full-report.pdf (accessed on 10 April 2023).
8. Huang, K.; Miller, J.B.; Huber, G.W.; Dumesic, J.A.; Maravelias, C.T. A general framework for the evaluation of direct nonoxidative methane conversion strategies. *Joule* **2018**, *2*, 349–365. [CrossRef]
9. Ramasubramanian, V.; Ramsurn, H.; Price, G.L. Methane dehydroaromatization—A study on hydrogen use for catalyst reduction, role of molybdenum, the nature of catalyst support and significance of Bronsted acid sites. *J. Energy Chem.* **2019**, *34*, 20–32. [CrossRef]
10. Karakaya, C.; Morejudo, S.H.; Zhu, H.; Kee, R.J. Catalytic chemistry for methane dehydroaromatization (MDA) on a bifunctional Mo/HZSM-5 catalyst in a packed bed. *Ind. Eng. Chem. Res.* **2016**, *55*, 9895–9906. [CrossRef]
11. Kosinov, N.; Coumans, F.J.A.G.; Uslamin, E.A.; Wijpkema, A.S.G.; Mezari, B.; Hensen, E.J.M. Methane dehydroaromatization by Mo/HZSM-5: Mono- or Bifunctional catalysis? *ACS Catal.* **2017**, *7*, 520–529. [CrossRef]
12. Menon, U.; Rahman, M.; Khatib, S.J. A critical literature review of the advances in methane dehydroaromatization over multifunctional metal-promoted zeolite catalysts. *Appl. Catal. A Gen.* **2020**, *608*, 117870. [CrossRef]
13. Beuque, A.; Hao, H.; Berrier, E.; Batalha, N.; Sachse, A.; Paul, J.-F.; Pinard, L. How do the products in methane dehydroaromatization impact the distinct stages of the reaction? *Appl. Catal. B Environ.* **2022**, *309*, 121274. [CrossRef]
14. Karakaya, C.; Zhu, H.; Kee, R.J. Kinetic modeling of methane dehydroaromatization chemistry on Mo/Zeolite catalysts in packed-bed reactors. *Chem. Eng. Sci.* **2015**, *123*, 474–486. [CrossRef]
15. Spivey, J.J.; Hutchings, G. Catalytic aromatization of methane. *Chem. Soc. Rev.* **2014**, *43*, 792–803. [CrossRef]
16. Kiani, D.; Sourav, S.; Tang, Y.; Baltrusaitis, J.; Wachs, I.E. Methane activation by ZSM-5-supported transition metal centers. *Chem. Soc. Rev.* **2021**, *50*, 1251. [CrossRef] [PubMed]
17. Pang, T.; Yang, X.; Yuan, C.; Elzatahry, A.A.; Alghamdi, A.; He, X.; Cheng, X.; Deng, Y. Recent advance in synthesis and application of heteroatom zeolites Author links open overlay panel. *Chin. Chem. Lett.* **2021**, *32*, 328–338. [CrossRef]

18. Sun, K.; Ginosar, D.M.; He, T.; Zhang, Y.; Fan, Y.; Chen, R. Progress in Nonoxidative Dehydroaromatization of Methane in the Last 6 Years. *Ind. Eng. Chem. Res.* **2018**, *57*, 1768–1789. [CrossRef]
19. Hartmann, M.; Machoke, A.G.; Schwieger, W. Catalytic test reactions for the evaluation of hierarchical zeolites. *Chem. Soc. Rev.* **2016**, *45*, 3313–3330. [CrossRef]
20. Feng, R.; Wang, X.; Lin, J.; Li, Z.; Hou, K.; Yan, X.; Hu, X.; Yan, Z.; Rood, M.J. Two-stage glucose-assisted crystallization of ZSM-5 to improve methanol to propylene (MTP). *Microporous Mesoporous Mater.* **2018**, *270*, 57–66. [CrossRef]
21. Parkhomchuk, E.V.; Sashkina, K.A.; Parmon, V.N. New heterogeneous catalysts based on zeolites with hierarchical pore system. *Pet. Chem.* **2016**, *56*, 197–204. [CrossRef]
22. Liu, H.; Yang, S.; Hu, J.; Shang, F.; Li, Z.; Xu, C.; Guan, J.; Kan, Q. A Comparison study of mesoporous Mo/H-ZSM-5 and conventional Mo/H-ZSM-5 catalysts in methane non-oxidative aromatization. *Furl Process. Technol.* **2012**, *96*, 195–202. [CrossRef]
23. Na, K.; Choi, M.; Ryoo, R. Recent advances in the synthesis of hierarchically nanoporous zeolites. *Microporous Mesoporous Mater.* **2013**, *166*, 3–19. [CrossRef]
24. Yang, K.; Zhou, F.; Ma, H.; Yu, L.; Wu, G. Glucose-Assisted Synthesis of Hierarchical HZSM-5 for Catalytic Fast Pyrolysis of Cellulose to Aromatics. *ChemistrySelect* **2021**, *6*, 11591–11598. [CrossRef]
25. Liu, H.; Kan, Q. Improved performance of hierarchical porous Mo/H-IM-5 catalyst in methane non-oxidative aromatization. *Appl. Petrochem. Res.* **2017**, *7*, 2–4. [CrossRef]
26. Liu, K.; Caglayan, M.; Dikhtiarenko, A.; Zhang, X.; Sayidov, O.; Abou-Hamad, E.; Gascon, J.; Chowdhury, A.D. Are hierarchical zeolites good catalysts for Methane Dehydroaromatization? A critical analysis. *Catal. Today* **2023**, *408*, 22–35. [CrossRef]
27. Dipak, B.S.; Viomesh, P.P. Estimation of crystalline phase in ZSM-5 zeolites by infrared spectroscopy. *J. Chem. Technol. Biotechnol.* **1989**, *44*, 147–154.
28. Bukhtiyarov, V.I.; Zaikovskii, V.I.; Kashin, A.S.; Ananikov, V.P. Modern electron microscopy in the study of chemical systems at the boundary of organic synthesis and catalysis. *Russ. Chem. Rev.* **2016**, *85*, 1198–1214. [CrossRef]
29. Vosmerikov, A.V.; Erofeev, V.I. Influence of mechanical treatment on the catalytic properties of zeolite-containing catalysts for aromatization of lower alkanes. *Russ. J. Phys. Chem. A* **1995**, *69*, 787–790.
30. Vosmerikov, A.V.; Korobitsyna, L.L.; Barabashin, Y.E.; Arbuzova, N.V.; Echevskii, G.V.; Kodenev, E.G.; Zhuravkov, S.P. Deactivation of Molybdenum-Containing Zeolites in the Course of Nonoxidative Methane Conversion. *Kinet. Catal.* **2005**, *46*, 724–728. [CrossRef]
31. Break, D.W. *Zeolite Molecular Sieves: Structure, Chemistry, and Use*; Wiley: Hoboken, NJ, USA, 1973; p. 771.
32. Mamonov, N.A.; Fadeeva, E.V.; Grigoriev, D.A.; Mikhailov, M.N.; Kustov, L.M.; Alkhimov, S.A. Metal/zeolite catalysts of methane dehydroaromatization. *Russ. Chem. Rev.* **2013**, *82*, 567–585. [CrossRef]
33. Xiong, Z.-T.; Zhang, H.-B.; Lin, G.-D.; Zeng, J.-L. Study of W/HZSM-5 based catalysts for dehydroaromatization of CH_4 in absence of O_2. II. Action of promoters Zn and Li. *Catal. Lett.* **2001**, *74*, 233–243. [CrossRef]
34. Ma, D.; Lu, Y.; Su, L.; Xu, Z.; Tian, Z.; Xu, Y.; Lin, L.; Bao, X. Remarkable improvement on the methane aromatization reaction: A highly selective and coking-resistant catalyst. *J. Phys. Chem. B* **2002**, *106*, 8524–8530. [CrossRef]
35. Zhao, K.; Jia, L.; Wang, J.; Hou, B.; Li, D. The influence of the Si/Al ratio of Mo/HZSM-5 on methane non-oxidative dehydroaromatization. *New J. Chem.* **2019**, *43*, 4130–4136. [CrossRef]
36. Baerlocher, C.; McCusker, L.B.; Olson, D.H. *Atlas of Zeolite Framework Types*, 6th ed.; Elsevier: Amsterdam, The Netherlands, 2007; p. 398.
37. Hu, J.; Wu, S.; Ma, Y.; Yang, X.; Li, Z.; Liu, H.; Huo, Q.; Guan, J.; Kan, Q. Effect of the particle size of MoO_3 on the catalytic activity of Mo/ZSM-5 in methane non-oxidative aromatization. *New J. Chem.* **2015**, *39*, 5459–5469. [CrossRef]

Disclaimer/Publisher's Note: The statements, opinions and data contained in all publications are solely those of the individual author(s) and contributor(s) and not of MDPI and/or the editor(s). MDPI and/or the editor(s) disclaim responsibility for any injury to people or property resulting from any ideas, methods, instructions or products referred to in the content.